

## UC Irvine

### UC Irvine Previously Published Works

**Title**

Protein crystal growth in microgravity.

**Permalink**

<https://escholarship.org/uc/item/5j25m6j9>

**Journal**

Science (New York, N.Y.), 246(4930)

**ISSN**

0036-8075

**Authors**

DeLucas, LJ  
Smith, CD  
Smith, HW  
[et al.](#)

**Publication Date**

1989-11-01

**DOI**

10.1126/science.2510297

**Copyright Information**

This work is made available under the terms of a Creative Commons Attribution License, available at <https://creativecommons.org/licenses/by/4.0/>

Peer reviewed

- p. 469; H. K. Mao, in *Simple Molecular Systems at Very High Density*, P. Loubeyre, A. Polian, N. Boccara, Eds. (Plenum, New York, 1989), p. 221.
17. An analysis of the structure of CsI below 200 GPa, including the mechanism of the transformation from B2 to the hcp-like structure, will be presented elsewhere (H. K. Mao *et al.*, in preparation).
  18. M. Ross and A. K. McMahan, *Phys. Rev. B* **21**, 1658 (1980).
  19. We acknowledge the invaluable assistance of D. E. Cox at beamline X-7A of the National Synchrotron

Light Source, Brookhaven National Laboratory. We thank N. C. Holmes, J. A. Moriarty, G. R. Gathers, and W. J. Nellis for providing information on the Pt equation of state. We also thank Q. Williams, R. Reichlin, and A. L. Ruoff for constructive comments on the manuscript. Supported by the National Science Foundation under grants EAR-8610068, EAR-8708127, EAR-8720326, and EAR-8817263 by the Carnegie Institution of Washington.

10 July 1989; accepted 22 September 1989

## Protein Crystal Growth in Microgravity

LAWRENCE J. DELUCAS, CRAIG D. SMITH, H. WILSON SMITH, SENADHI VIJAY-KUMAR, SHOBHA E. SENADHI, STEVEN E. EALICK, DANIEL C. CARTER, ROBERT S. SNYDER, PATRICIA C. WEBER, F. RAYMOND SALEMME, D. H. OHLENDORF, H. M. EINSPAHR, L. L. CLANCY, MANUEL A. NAVIA, BRIAN M. MCKEEVER, T. L. NAGABHUSHAN, GEORGE NELSON, A. MCPHERSON, S. KOSZELAK, G. TAYLOR, D. STAMMERS, K. POWELL, G. DARBY, CHARLES E. BUGG

**The crystals of most proteins or other biological macromolecules are poorly ordered and diffract to lower resolutions than those observed for most crystals of simple organic and inorganic compounds. Crystallization in the microgravity environment of space may improve crystal quality by eliminating convection effects near growing crystal surfaces. A series of 11 different protein crystal growth experiments was performed on U.S. space shuttle flight STS-26 in September 1988. The microgravity-grown crystals of  $\gamma$ -interferon D<sup>1</sup>, porcine elastase, and isocitrate lyase are larger, display more uniform morphologies, and yield diffraction data to significantly higher resolutions than the best crystals of these proteins grown on Earth.**

**P**ROTEIN CRYSTALLOGRAPHY REQUIRES crystals of suitable size and quality for high-resolution diffraction analyses. A new development in protein crystal growth involves studies of crystal growth processes in the microgravity environment obtainable in space (1, 2). The major motivation behind these space experiments is to eliminate the density-driven convective flow that accompanies crystal growth in gravitational fields (3, 4). In

addition, sedimentation of growing crystals, which can interfere with the formation of single crystals, is eliminated in the absence of gravity.

Microgravity protein crystal growth experiments performed on Spacelab 1 by Littke and John (5) indicated that the space-grown crystals from a liquid-liquid diffusion system were larger than crystals obtained by the same experimental system on Earth. Experiments on four U.S. space shuttle missions in 1985 and 1986 led to development of an apparatus for protein crystal growth by vapor diffusion techniques (6). We used this equipment for a series of protein crystal growth experiments on U.S. space shuttle flight STS-26 in September 1988. The results of these experiments are presented.

The vapor diffusion technique used on STS-26 is closely related to the hanging drop method (7), and thus the microgravity results can be compared with extensive data obtained from experiments on Earth. The hardware was adapted from that used on a series of four shuttle missions in 1985 and 1986 (6). Crystals were grown in 40- $\mu$ l droplets that were extruded from syringes and subsequently permitted to equilibrate with solutions of precipitating agents con-

tained within closed chambers. Each experiment was performed within a chamber (5.3 cm<sup>3</sup>) with clear plastic windows. Before the launch, a double-barreled syringe was loaded with protein solution and crystallizing (precipitating) solutions in adjacent barrels. The mouths of these double-barreled syringes were stoppered during launch and landing. The chamber contained an absorbent material that was saturated with a solution of the precipitating agent. All solutions were loaded ~24 hours before the launch. Once in orbit, crystal growth was activated by extruding the solutions onto the tip of the syringe, where mixing of the protein solution and precipitating agent was achieved by repeatedly withdrawing and extruding the solutions. The suspended droplet was then allowed to equilibrate with the surrounding solution of precipitating agent. The protein droplets were photographed after activation and at 24-hour intervals during the 3-day experiments. After 3 days, the solutions and suspended crystals were withdrawn into the syringes and stoppered for return to Earth (8).

Control experiments on Earth were performed in equipment identical to that used for the shuttle experiments. The control experiments were begun 7 days after the shuttle landed; the same protein solutions and identical loading, activation, and deactivation times were used in the control experiments as in the STS-26 experiments. Extensive control experiments were also performed in prototypes of the space shuttle hardware before and after the shuttle experiments were completed.

X-ray diffraction photographs were used for qualitative evaluation of diffraction resolutions. The results from these analyses are consistent with the more detailed studies of three-dimensional (3-D) data sets measured with the area detector systems (9). Because evaluation of diffraction resolutions from photographs is highly subjective, and is often dependent on crystal orientations, we have depended primarily on 3-D intensity data sets for comparison of space- and Earth-grown crystals.

Intensity data sets from crystals of three proteins were analyzed in a variety of different ways (Fig. 1). The largest Bragg angles at which usable data could be measured were assembled, and the percentage of data above background levels throughout the data collection range was evaluated. Plots were made of average  $I/\sigma(I)$  values, where  $I$  is intensity, versus diffraction resolution and of percentages of data above various cutoff levels as functions of resolution. Data sets from space- and Earth-grown crystals were compared by using Wilson plots (10). The Wilson plot can be used to estimate the

L. J. DeLucas, C. D. Smith, H. W. Smith, S. Vijay-Kumar, S. E. Senadhi, S. E. Ealick, C. E. Bugg, University of Alabama at Birmingham, Center for Macromolecular Crystallography, Birmingham, AL 35294.  
D. C. Carter and R. S. Snyder, George Marshall Space Flight Center, Huntsville, AL 35812.  
P. C. Weber, F. R. Salemme, D. H. Ohlendorf, E. I. du Pont de Nemours & Company, Central Research and Development Department, Wilmington, DE 19880.  
H. M. Einspahr and L. L. Clancy, Upjohn Company, Kalamazoo, MI 49001.  
M. A. Navia and B. M. McKeever, Merck Sharp & Dohme Research Laboratories, Rahway, NJ 07065.  
T. L. Nagabhushan, Schering-Plough Corporation, Bloomfield, NJ 07003.  
G. Nelson, Astronomy Department, University of Washington, Seattle, WA 98195.  
A. McPherson and S. Koszelak, University of California at Riverside, Riverside, CA 92521.  
G. Taylor, Laboratory of Molecular Biophysics, University of Oxford, Oxford OX1 3QU, United Kingdom.  
D. Stammers, K. Powell, G. Darby, Wellcome Research Laboratories, Beckenham BR3 3BS, United Kingdom.

overall  $B$  values for a crystal, the  $B$  value being a parameter that reflects the internal order within a crystal. Relative Wilson plots, also known as difference Wilson plots (10), are useful for assessing changes in the internal order of protein crystals. These plots of  $\ln(\Sigma F_a^2 / \Sigma F_b^2)$ , where  $F$  is the crystallographic structure factor for crystals of type  $a$  and  $b$ , versus  $4 \sin^2 \theta / \lambda^2$  (resolution) are routinely used to characterize and compensate for the disordering effects resulting from the diffusion of heavy-atom derivatives into protein crystals. The slopes of these plots are directly related to the difference in overall  $B$  values for two different crystals, a (Earth-grown) and  $b$  (space-grown).

The STS-26 experiments included an engineered native form of  $\gamma$ -interferon D<sup>1</sup> ( $\gamma$ -IFN D<sup>1</sup>). Crystals of  $\gamma$ -IFN D<sup>1</sup> are trigonal (space group  $R32$ , with  $a = b = 114 \text{ \AA}$  and  $c = 315 \text{ \AA}$ ). The crystals were grown from a

solution of 49% ammonium sulfate, 0.05M sodium acetate,  $pH = 5.9$  (11). Many crystallization experiments were performed at the University of Alabama at Birmingham with this protein over a 2-year period, and 3-D intensity data sets were collected. For STS-26, five crystallization experiments were performed under conditions identical, except for gravity, to those routinely used for crystal growth studies on Earth. Two crystals were obtained that were larger than the best that have been produced in any ground experiments; one was  $\sim 50\%$  larger than the largest crystal that had been obtained previously. The overall morphology was similar to the Earth-grown crystals.

The 3-D intensity data for the STS-26 crystal were compared with data sets obtained from four Earth-grown crystals. The space-grown crystal displayed an increase in measurable data throughout the resolution

range, with a significant fraction of measured data beyond  $3.0 \text{ \AA}$  resolution, where the Earth-grown crystals displayed no significant diffraction.

Although this improvement could reflect enhanced counting statistics resulting from the larger crystal volume, examination of a relative Wilson plot indicated that the space-grown crystal has a lower effective  $B$  value. This relative Wilson plot is shown in Fig. 2A, where the data from the space-grown crystal is scaled to the data from an Earth-grown crystal. If the  $B$  values of the two crystals were comparable, the relative Wilson plot should be flat with a slope of zero. For comparative purposes, a Wilson plot based on data from two of the Earth-grown  $\gamma$ -IFN D<sup>1</sup> crystals is shown. The slope for this plot is essentially zero, whereas the space versus ground plot displays a positive slope throughout the resolution range, with a steeper slope at the higher resolutions, indicating that the  $B$  value for the space-grown crystal is lower than that for the Earth-grown crystal.

Crystals of porcine elastase are orthorhombic (space group  $P2_12_12_1$ , with  $a = 50.9 \text{ \AA}$ ,  $b = 57.2 \text{ \AA}$ , and  $c = 75.0 \text{ \AA}$ ). Crystals were grown by seeding techniques from solutions of precipitant (1.5M sodium sulfate, 0.1M sodium acetate,  $pH = 5.0$ ) (12). Small seed crystals were added to the solution of precipitating agent in one side of the double-barreled syringes. The seed crystals used were  $\sim 50 \text{ \mu m}$  in the maximum dimension. A number of well-formed elastase crystals in the range of 0.5 to 2.1 mm were obtained from six crystallization experiments on STS-26. Comparison of 3-D intensity data for a space-grown crystal with dimensions comparable to Earth-grown crystals studied earlier (13) (Fig. 1B) revealed that the space-grown crystal yielded significantly more data at all resolution ranges, with enhancement in the ultimate resolution at which measurable data can be obtained. The relative Wilson plot (Fig. 2) did not reveal a significant difference in  $B$  values for data in the lower resolution ranges, but the higher resolution data indicated that the space-grown crystal had a significantly lower overall effective  $B$  value.

Crystals of isocitrate lyase are orthorhombic (space group  $P2_12_12_1$ , with  $a = 80.7 \text{ \AA}$ ,  $b = 123.1 \text{ \AA}$ , and  $c = 183.4 \text{ \AA}$ ). Crystals are grown from a solution of 1.7M sodium citrate, 0.1M tris-HCl,  $pH = 8.0$ . Crystallization experiments (14) have invariably resulted in the growth of dendritic clusters (Fig. 3A).

An improved habit for isocitrate lyase was observed from the experiments on STS-26. Although some dendritic growth was found in the space samples, a number of well-

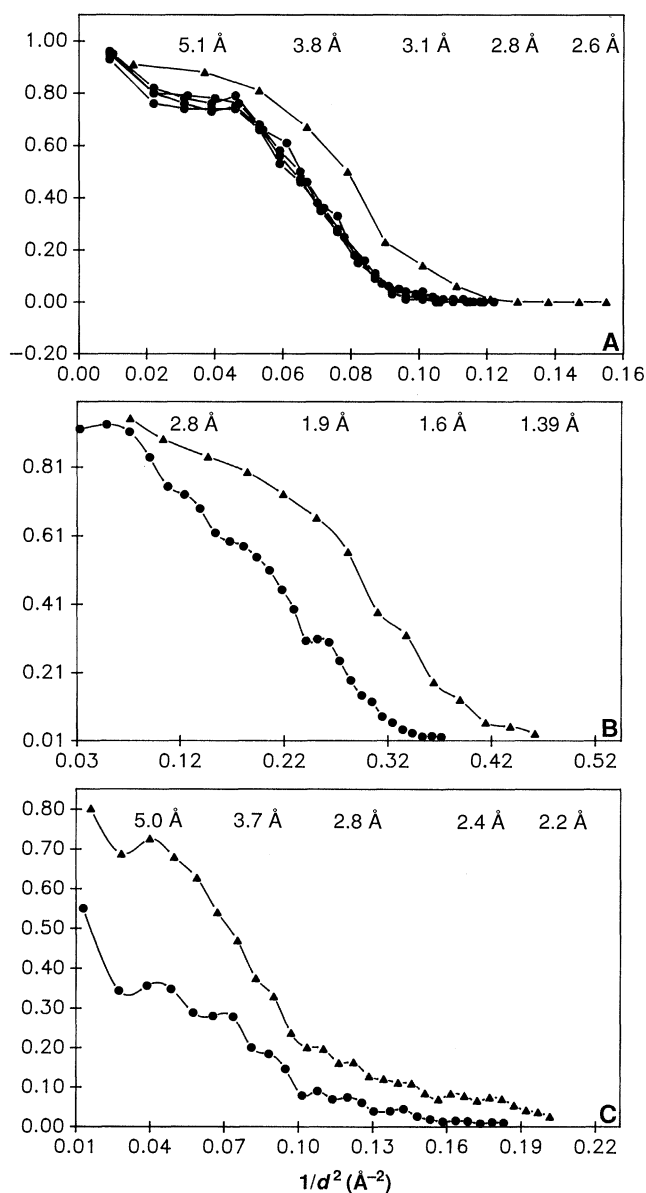


**Fig. 1.** Comparison of diffraction intensity data for space-grown ( $\blacktriangle$ ) and Earth-grown ( $\bullet$ ) crystals of (A)  $\gamma$ -IFN D<sup>1</sup>, (B) porcine elastase, and (C) isocitrate lyase. The  $y$  axis shows the fraction of data with  $I/\gamma(I) \geq 5$ . (A) Space-grown  $\gamma$ -IFN D<sup>1</sup> crystal and the data obtained from four of the largest Earth-grown crystals of  $\gamma$ -IFN D<sup>1</sup>. (B) Space-grown porcine elastase crystal and a porcine elastase crystal of comparable size grown on Earth. (C) Comparison of intensity distributions for space-grown and Earth-grown crystals of isocitrate lyase.

formed prisms (Fig. 3B) were obtained. These prisms belong to the same space group as the Earth-grown dendrites, but they yielded better intensity data throughout the intensity range (Fig. 1C). A relative Wilson plot (Fig. 2C) indicated that, except at the lowest resolution range, the space-grown crystal had a significantly lower effective  $B$  value than the Earth-grown crystal.

Of the eight other proteins crystallized on STS-26 (15), six did not produce crystals large enough for diffraction analysis. One produced only a partial data set, the analysis of which was inconclusive when compared to Earth data. The final protein (canavalin) displayed higher resolution ( $\sim 0.2 \text{ \AA}$ ) on the film data, but the 3-D data could not be processed because of experimental difficulties that arose during the data collection process.

The improved diffraction patterns from the space-grown crystals may not be entirely attributable to enhanced internal order of the crystals. Intensity data sets were collected in three different laboratories in order to obtain the data as rapidly as possible after the space experiments and to collect data at

locations where Earth-grown crystals were routinely analyzed. Although the same type of area detector system was used in these three laboratories, there were variations in data collection procedures. However, when the results for these experiments are considered together, the data indicate that protein crystals grown under microgravity conditions diffract to higher resolution than the best crystals obtained under similar conditions on Earth. The lack of success for six of the eight remaining proteins is attributed to nonoptimum crystal growth conditions for the space experiment.

The relative Wilson plots indicate that the space-grown crystals are more highly ordered at the molecular level than crystals grown by the same method on Earth. Under microgravity conditions, convective flow patterns that accompany crystal growth would be eliminated, thus generating a more controlled environment at crystal interfaces. Because protein crystals are relatively weakly bonded, with water bridges playing predominant roles, molecular-packing patterns may be more regular in the absence of convective turbulence. The ability

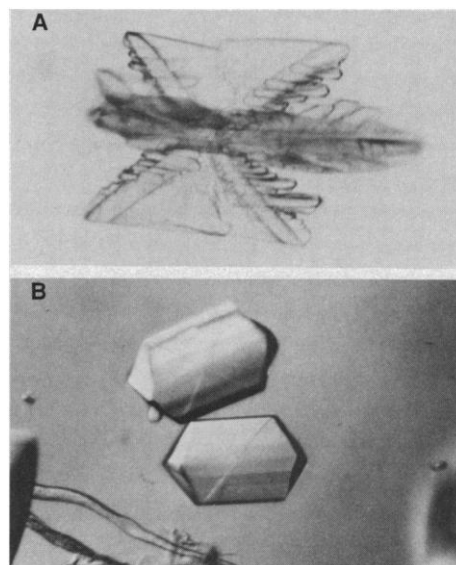


**Fig. 3.** (A) Typical dendritic morphology for isocitrate lyase crystals grown on Earth. The dimensions of this dendritic cluster are 0.74 and 0.46 mm, respectively. (B) Prisms of isocitrate lyase grown on STS-26. The crystal dimensions are approximately 0.4 mm by 0.25 mm by 0.4 mm.

to grow protein crystals with increased molecular order should enhance crystallographic solutions by shortening the time required to determine the structure and by increasing the accuracy of molecular details.

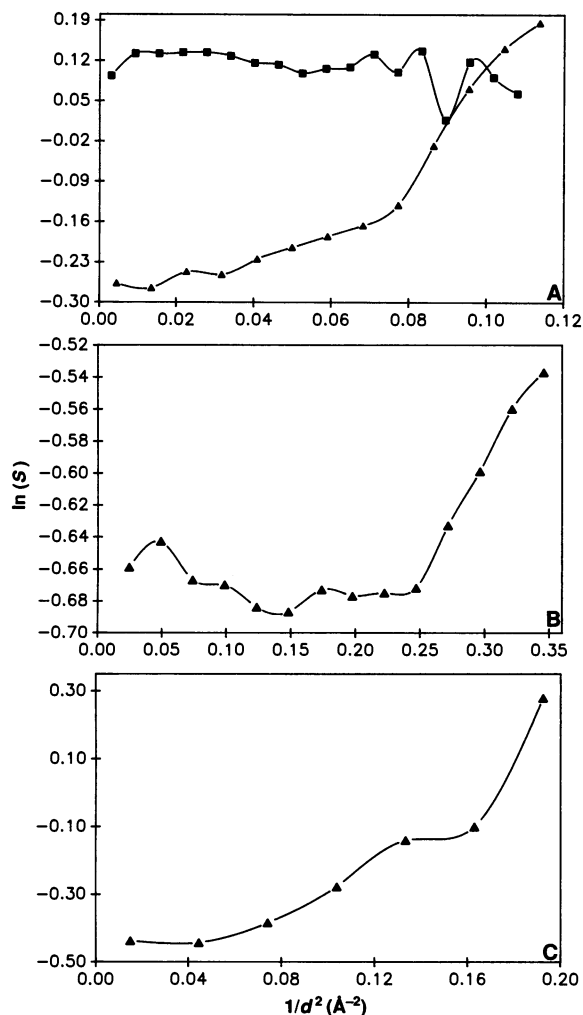


**Fig. 2.** Relative Wilson plot ( $\blacktriangle$ ) comparing space-grown and Earth-grown crystals of (A)  $\gamma$ -IFN D<sup>1</sup>, (B) porcine elastase, and (C) isocitrate lyase. In addition, a relative Wilson plot ( $\blacksquare$ ) comparing two Earth-grown crystals of  $\gamma$ -IFN D<sup>1</sup> is shown in (A).  $S = \sum F_a^2 / \sum F_b^2$ .

#### REFERENCES AND NOTES

1. L. J. DeLucas and C. E. Bugg, *Trends Biotechnol.* **76**, 188 (1987).
2. C. E. Bugg, *J. Cryst. Growth* **76**, 535 (1986).
3. M. Pusey, W. Witherow, R. Naumann, *ibid.* **90**, 105 (1988).
4. R. L. Kroes and D. Reiss, *ibid.* **69**, 414 (1984).
5. W. Litke and C. John, *Science* **225**, 203 (1984).
6. L. J. DeLucas *et al.*, *J. Cryst. Growth* **76**, 681 (1986).
7. A. McPherson, *Methods Enzymol.* **114**, 112 (1985).
8. The experimental apparatus was contained within a temperature-controlled module that was maintained at  $22.8 \pm 0.7^\circ\text{C}$  from the time that the samples were loaded until the analyses of the crystals could be performed. Slightly higher temperatures occurred for short periods of time during the photographic sessions. Immediately after the shuttle landed, the hardware was transported in the incubator to Birmingham, Alabama, where the analyses were initiated. The space-grown crystals were extruded into depression plates, sealed with glass cover slips, and photographed with the use of a binocular microscope. Selected crystals were sealed in glass capillaries for x-ray diffraction analysis.
9. X-ray diffraction photographs were obtained with crystals in stationary orientations by the use of specially constructed cylindrical cassettes mounted on rotating anode x-ray generators. More detailed x-ray diffraction studies were performed with Nicolet area detector systems [A. J. Howard *et al.*, *J. Appl. Crystallogr.* **20**, 383 (1987)] mounted on rotating anode x-ray generators with copper targets, at the University of Alabama at Birmingham (for  $\gamma$ -IFN D<sup>1</sup> and canavalin), du Pont (for isocitrate lyase), Merck (for porcine elastase), and the Marshall Space Flight Center (for human serum albumin).
10. T. L. Blundell and L. N. Johnson, *Protein Crystallography* (Academic Press, New York, 1976), pp. 333–336.
11. S. Vijay-Kumar *et al.*, *J. Biol. Chem.* **262**, 4804

- (1987).
12. L. Sawyer *et al.*, *J. Mol. Biol.* **18**, 137 (1978).
  13. M. A. Navia and B. M. McKeever, unpublished data.
  14. P. C. Weber, F. R. Salemme, D. H. Ohlendorf, unpublished data.
  15. Canavalin, human serum albumin, human C-reactive protein, snake venom phospholipase A<sub>2</sub>, human renin, synthetic peptide, human purine nucleoside phosphorylase, and human immunodeficiency virus reverse transcriptase.

16. Supported by NASA contract NAS8-36611 and NASA grant NAGW-813. We thank D. Jex, R. Naumann, members of Teledyne-Brown Engineering Company who designed and constructed our protein crystal growth apparatus, the many NASA employees who helped at all stages of the shuttle activities, and F. Suddath for invaluable assistance in developing a space version of the hanging drop method.

25 May 1989; accepted 29 August 1989

## Proton Motive Force Involved in Protein Transport Across the Outer Membrane of *Aeromonas salmonicida*

KEVIN R. WONG AND J. THOMAS BUCKLEY\*

Many Gram-negative bacteria export proteins to the exterior. Some of these proteins are first secreted into the periplasm and then cross the outer membrane in a separate step. The source of energy required for the translocation is unknown. Export of the extracellular protein proaerolysin from the periplasm through the outer membrane of *Aeromonas salmonicida* is inhibited by a proton ionophore and by low extracellular pH. One possible explanation of these results is that a proton gradient across the outer membrane is required for export.

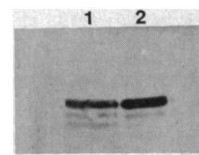
THE OUTER MEMBRANE OF GRAM-negative bacteria is thought to be a rather inert structure that allows the free movement of small molecules through holes created by porins but forms a barrier to large molecules like proteins (1). Yet this membrane must be crossed by proteins that are released into the culture supernatant by the Gram-negative species capable of export. The mechanisms used to accomplish this have received little attention, in part because *Escherichia coli* does not appear to have a general extracellular secretory system. Release of proteins by this species requires the participation of other gene products or results from rupture of the outer membrane (2).

The limited evidence available from research with other species suggests that two general pathways are followed during protein export (3). In the first, the two membranes appear to be crossed simultaneously, at zones of adhesion. This pathway would seem to be the least complicated and most direct, yet of those proteins studied, only exotoxin A of *Pseudomonas aeruginosa* is said to be released in this way (4). Other proteins traverse the inner and outer membranes in separate steps, entering the periplasm during transit. Two examples are proaerolysin, the precursor of the hemolytic toxin of

*Aeromonas hydrophila* (5), and choleraen of *Vibrio cholerae* (6). Like outer membrane and periplasmic proteins, they first cross the inner membrane, and their signal sequences are removed before they are released into the periplasm. From there they somehow cross the outer membrane and appear in the culture supernatant as water-soluble proteins. How they get through the outer membrane is not understood. Although there are large concentration gradients between the periplasm and the exterior for both proaerolysin in *A. hydrophila* and choleraen in *V. cholerae*, it is hard to imagine how the concentration of the proteins could be enough to drive them across the outer membrane. Nor can transfer be a consequence of covalent modification, as the periplasmic forms of both proteins are functionally and physically indistinguishable from the forms isolated from the culture supernatants.

The secretion of proteins across the inner bacterial membrane requires an electrochemical gradient (7). Membrane potentials and chemical gradients of protons are not usually considered as potential driving forces for protein export, however, because the holes formed by porins in the outer membrane are believed to allow free movement of small molecules. Nevertheless, there is some evidence that an appreciable electrical potential can exist across the outer membrane of *E. coli* because of the large concentration of negative charges in the periplasm, and it is estimated that the pH of the periplasm should be significantly lower than the pH of the exterior medium (8).

**Fig. 1.** Molecular form of intracellular aerolysin. *A. salmonicida* AS440 (ATCC 14174) containing the plasmid pKW2 (10) was grown at 27°C to an optical density at 600 nm ( $OD_{600}$ ) of 2.4 in LB. The cells were centrifuged and immediately resuspended in the sample buffer used in sodium dodecyl sulfate electrophoresis (15) and boiled. After electrophoresis, the proteins were transferred to nitrocellulose and immunoblotted with a mouse monoclonal antibody to aerolysin (16): lane 1, total cell contents; lane 2, purified proaerolysin. Identical results were obtained with rabbit polyclonal antibody to aerolysin.



Recently we cloned the structural gene for proaerolysin into *A. salmonicida* (9). The protoxin is exported from the bacteria to the culture supernatant, and during export it is possible to measure a pool of cell-associated proaerolysin. Most of this pool can be recovered by osmotic shock, indicating that it is periplasmic, although it may be weakly associated with one of the membranes. When the bacteria are transferred to fresh medium containing chloramphenicol (to prevent the synthesis of new protein), time-dependent release of the protoxin results. Here we use this system to study the mechanism of transfer of proaerolysin across the outer membrane of *A. salmonicida*.

In the first experiment, bacteria were grown in LB medium at pH 7.5. The results in Fig. 1 show that no preprotoxin could be detected in the cells, indicating that the signal sequence had been removed. This is further evidence that most of the proaerolysin found in these cells has crossed the inner membrane. When the cells were transferred to fresh media containing chloramphenicol, the shockable pool of proaerolysin was rapidly depleted, resulting in the appearance of the protoxin in the medium (Fig. 2) as we have found earlier. The results in Fig. 2 also show that release of proaerolysin was virtually completely inhibited by the presence of the proton ionophore carbonyl cyanide *m*-chlorophenyl hydrazone (CCCP) in the new media. The most obvious interpretation of this result is that export of proaerolysin across the outer membrane is somehow coupled to the electrochemical gradient across the inner membrane and that the gradient is dissipated by CCCP. Such a system, which involves TonB and other proteins, is said to be required for the import of colicins and some nutrients across the outer membrane of *E. coli* (10).

Another possibility is that CCCP abolishes a proton gradient across the outer membrane that is required for proaerolysin export. If this were the case, then reducing the size of the gradient by lowering the pH of

Department of Biochemistry and Microbiology, University of Victoria, Victoria, BC, Canada, V8W 2Y2.

\*To whom correspondence should be addressed.